

# Modelling Renewable Energy Sources for Harmonic Assessments in DIgSILENT PowerFactory: Comparison of Different Approaches

Zhida Deng<sup>1</sup><sup>a</sup>, Grazia Todeschini<sup>1</sup><sup>b</sup>, Kah Leong Koo<sup>2</sup><sup>c</sup> and Maxwell Mulimakwenda<sup>2</sup><sup>d</sup>

<sup>1</sup>Faculty of Science and Engineering, Swansea University, Swansea, U.K.

<sup>2</sup>Power Quality and Modelling Department, National Grid, Warwick, U.K.


**Keywords:** Harmonics, Power Quality, Power Systems Modelling, Renewable Energy Sources, Total Harmonic Distortion, Voltage Unbalance.


**Abstract:** With the increasing number of Renewable Energy Sources connected to the power grid, the impact on system operation is becoming more evident. To assess this impact, accurate computer models are required for both the power system and the devices connected to it. Various types of system integration studies need to be performed in order to study both steady-state and abnormal operation. Among the steady-state analyses, power quality studies assess the impact of Renewable Energy Sources on parameters such as voltage levels and harmonic content. Harmonic studies are gaining more attention because of the nature of renewable energy sources which are mainly connected to the power grid through electronic power converters, thus producing undesirable harmonics. This paper analyses various settings, solvers and harmonic source models in a commercial software – DIgSILENT PowerFactory – to ensure accurate calculation and correct interpretation of harmonic assessment. A simple model comprising seven harmonic devices is used for the analysis of various case studies. Their results are then compared with the standard IEC model and recommendations are proposed on how to appropriately model the RESs depending on the specific application considered.


## 1 INTRODUCTION


Existing power systems were designed decades ago when fossil fuels (e.g. coal, gas, oil) were exclusively employed to generate electricity. With growing population and industrial expansion, has led to increasing demands on power systems pushing them closer to their operational limits. Challenges to reduce greenhouse gases from conventional power stations to tackle climate change have also raised more serious concerns on the sustainability of fossil fuel-based power generation. These concerns have fueled the development of Renewable Energy Sources (RESs) to meet future electricity demands and displace conventional generations. It is expected that RESs will make up to approximately 63.15% of total installed generation capacity by 2050 in the UK, according to the National Grid Future Energy Scenarios report (National Grid ESO, 2019).

Since conventional power systems have not been designed to operate not only with large number of RES devices but also of increasing capacities, power quality issues need to be managed to an acceptable level. Increasing harmonic levels is identified as one of the main areas of concern in relation to RESs integration, and needs to be well studied and properly managed, as reported in (Working Group JWG-C4/C6.29, 2016). The voltage and current are sinusoidal waveforms in an ideal Alternating Current (AC) power system but are distorted by harmonics that are produced by nonlinear loads and power electronic-based devices, for example motor drives and RES inverter (IEEE Power and Energy Society, 2014). These devices produce harmonics at multiple or sub-multiple integers of fundamental frequency. Small levels of harmonics are tolerated by equipment and various standards have been developed for harmonic control and to manage their connection to the network (Energy Networks Association, 2020;

<sup>a</sup> <https://orcid.org/0000-0002-8448-1934>

<sup>b</sup> <https://orcid.org/0000-0001-9411-0726>

<sup>c</sup> <https://orcid.org/0000-0002-9549-8627>

<sup>d</sup> <https://orcid.org/0000-0001-9433-4607>

IEC TR 61000-3-6, 2008; IEEE Power and Energy Society, 2014). This is because excessive harmonic levels may lead to various detrimental effects, including dielectric failure, overheating of electrical equipment, and false operation of circuit breakers (Cherian et al., 2016). Since RESs are mainly based on the use of power electronics, they inject harmonics into the network. With rapidly increasing number of these devices, even if individual units are compliant with the standards, the combined effect of numerous RESs installed in close proximity will lead to an overall increase of harmonic levels in the system (Koo & Emin, 2016).

Computer simulations are used to assess the impact of RESs on harmonic levels on the network. Both time-domain and frequency-domain methods are used (Medina et al., 2013). Time-domain methods characterise system behaviour using differential equations, and individual harmonic components can be derived via Fourier transformation. Although these methods provide detailed and accurate models of non-linear devices and their control algorithms, they do not allow easy calculation of the system impedances as well as modelling of the frequency-dependent parameters (Medina et al., 2013).

Frequency-domain analysis methods, including frequency scans, harmonic penetration studies and harmonic load flows, are widely employed in engineering practices to predict expected harmonic distortions on the network. By performing frequency-domain analysis, harmonic current and voltage distortions on the network as well as resonances are calculated. This process allows assessing compliance with the standards and, if required, informs on requirements for the filter design (Working Group JWC-C4/B4.38, 2019). A frequency scan consists of calculation of network impedance at various frequencies to determine frequency responses of power system and identify potential resonance conditions; a harmonic penetration study refers to nodal analysis for each harmonic order assuming no interaction between fundamental and harmonic components; a harmonic load flow uses Newton-Raphson or Gauss-Seidel based algorithm to solve unified fundamental and harmonic power flow equations, as described in (Herraiz et al., 2003; Medina et al., 2013). It is important to observe that in practice, the terms ‘harmonic load flow’ and ‘harmonic penetration studies’ are often used interchangeably, but these approaches may produce different results. Hence, it is important to understand the assumptions underlying the software and the solver under consideration.

Frequency-domain analysis can be carried out for balanced and unbalanced systems. In practical power systems, unbalance between phases is small from asymmetry in transmission systems and the nature of the loads and generating sources are normally unbalanced, therefore a balanced frequency-domain analysis is generally sufficient. However, unbalanced harmonic analysis provides more accurate results when studying asymmetrical systems, either in terms of network configuration (Jensen, 2018), and/or loads. In power systems where RESs are single-phase connected, it may be necessary to consider unbalance harmonic distribution between the phases in order to carry out a more accurate assessment.

In addition to unbalance, the summation of harmonics due to different sources and harmonic source modelling is an important factor that will also have an impact on the accuracy of the results. For harmonic summation, two approaches are mainly used: (1) either the magnitude and phase are considered for each harmonic component, (2) or the summation rule described in standard IEC 61000-3-6 (IEC TR 61000-3-6, 2008) is employed. In the latter case, a summation exponent is considered to take into account harmonic phase angles at higher harmonic orders. While IEC summation rule is based on practical considerations, it may result in inaccurate assessment of harmonic level at the Point of Common Coupling (PCC) (Eltouki et al., 2018; Working Group JWG-C4/C6.29, 2016) – i.e. at the point where multiple loads or sources connect to the system. This discrepancy may be due to the harmonic components adding or cancelling to varying degrees due to the harmonic phase angle differences, where this phenomenon may not be taken into account accurately when applying the IEC summation rule. As in (Ghassemi & Koo, 2010), different modelling approaches are described to calculate the harmonic distortion at the PCC for an offshore wind farm, and the limitations of the IEC summation rule are highlighted.

With large penetration of power converters, such as the ones used for RESs, it is more likely that harmonic phase angles will be randomly varying within a reasonable range (Bećirović et al., 2018). Under these conditions, it is more appropriate to carry out harmonic analysis by varying the harmonic phase angles to provide a more realistic harmonic assessment. Although the topic of harmonic assessment for RESs is not new, not many research works can be found considering the impact of IEC summation rule, appropriate use of harmonic models, and system unbalance conditions at the same time.

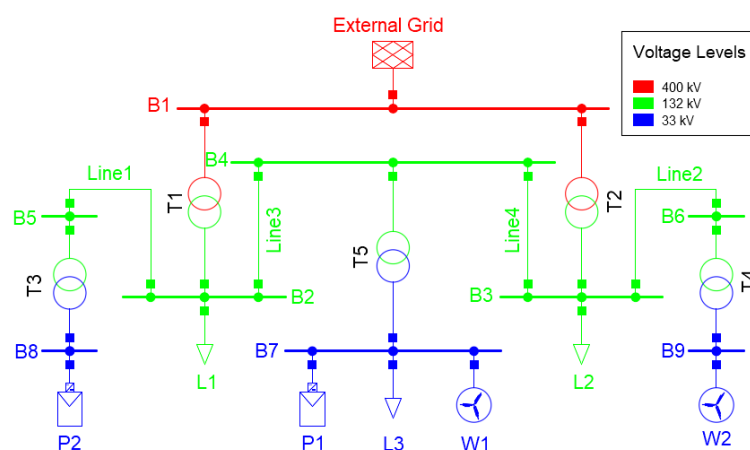


Figure 1: Single-line diagram of the simulated network.

The commercial software – DIgSILENT PowerFactory (DPF) (DIgSILENT, 2020a) – is widely used to perform power quality assessments and provides numerous options to carry out harmonic analysis. These options include: harmonic source models (named IEC source and Unbalance Phase Correct source), summation rules and solvers. If these options are not used appropriately to model the actual equipment, results may vary significantly, thus leading to misleading harmonic assessments. Although the user manual (DIgSILENT, 2020b) briefly explains the differences between these options, it is not clear enough to understand their impact on the harmonic assessment.

This work aims at examining the appropriate use of different harmonic source models and choice of harmonic load flow solvers available within DPF to calculate harmonic levels in distribution and transmission systems. This paper provides a better understanding of using different options in DPF and modelling guidance for unbalanced harmonic current sources in a way that allows flexibility while at the same time providing comparable results as the ones provided by the IEC model. DPF is used here as it is a widely used software in the power industry and similar concerns may arise with other software.

A simple 9-bus network with 7 harmonic sources is considered: the network is symmetrical in nature, and unbalance is caused by the harmonic sources only. Future work will address unbalanced networks. In Section 2, the network and harmonic source models are described. In Section 3, three test cases with different number of harmonic sources are set up for harmonic analysis. The frequency scans and voltage Total Harmonic Distortions (THDs) obtained from different solvers and harmonic source models are compared and discussed. Finally, the possibility

of matching IEC harmonic current source model using equivalent Unbalanced Phase Correct (UPC) model is investigated.

## 2 SIMULATION NETWORK AND HARMONIC SOURCE

### 2.1 Network Description

A 50 Hz symmetrical three-phase 9-bus network – including 4 transmission lines, two photovoltaics (PV) plants, 2 Wind Turbine Generator (WTGs), 3 Loads and 5 two-winding Wye grounded-delta (Yg-d) connected transformers with 30-degree phase shift was built in DPF, as shown in Figure 1. To ensure convergence of the power flow at fundamental frequency, an external grid element acting as slack bus was used. Distributed-parameter line model was adopted to consider the long-line effects (i.e. higher frequencies increase the electrical distance of the line (Working Group JWC-C4/B4.38, 2019)) during the harmonic analysis. The voltage levels are indicated by different colours, and the system component specifications and power flow parameters are given in Table 1.

### 2.2 Harmonic Source Modelling

In this paper, two constant harmonic current source models available in DPF – UPC and IEC – were considered. Harmonic current amplitudes (referred to the fundamental current) up to the 50<sup>th</sup> harmonic order found from the literature for loads (Preda et al., 2012; Robinson, 2003), PV farms (Elkholy, 2019; Erik & Leigh, 2016; Oliver et al., 2018; Rampinelli et

Table 1: System component parameters.

	L1	L2	L3	P1	P2	W1	W2
$S_r$ (MVA)	20	30	100	12	21	60	30
$P$ (MW)	19	28.5	90	8	18	40	20
$Q$ (Mvar)	6.25	9.37	43.59	0	0	0	0
	T1 – T2			T3 – T5			
Voltage	400/132 kV			132/33 kV			
$S_r$ (MVA)	255			90			
$Z$	16% short-circuit voltage with 1.8 MW losses			13% short circuit voltage with 0.25 MW losses			
	Line1	Line2	Line3	Line4			
$L$ (km)	15	20	24	31			
$Z$ ( $\Omega$ /km)	positive/negative-sequence R and X: 0.0212 and 0.1162;						
	zero-sequence R and X: 0.0848 and 0.4650						
	External Grid						
	Short-circuit power: 10000 MVA;						
	short circuit current: 14.43 kA; c-factor: 1.1;						
	R/X ratio: 0.1, R: 1.75 $\Omega$ , X: 17.51 $\Omega$						

Note that the symbols  $S_r$ ,  $P$ ,  $Q$ ,  $Z$ ,  $R$ ,  $X$  and  $L$  denote rated power, active power, reactive power, impedance resistance, reactance, and line length, respectively.

al., 2015) and wind farms (Ambrož et al., 2017; Energyforsk, 2018; Mendonça et al., 2012; Preciado et al., 2015; Rauma, 2012) are given in Table 2. The harmonic data for WTG at 42-50 orders is reported as smaller than 0.1 in (Ambrož et al., 2017): without loss of generality, the value of 0.1 was used in this paper.

Since the harmonic current injection for the IEC harmonic model in DPF can only be based on the rated current, the rated current ( $I_r$ ) was chosen as the reference current for the UPC model to ensure the same amount of harmonic current injections as the IEC model. For modelling the IEC harmonic current source, the data given in Table 2 were used as harmonic current injections and the standard IEC or self-defined summation rule can be selected to take into account the harmonic phase angles. The standard IEC summation rule is expressed as (IEC TR 61000-3-6, 2008):

$$I_h = \sqrt[\alpha]{\sum_{i=1}^N (I_h^i)^\alpha} \quad (1)$$

$$\alpha = \begin{cases} 1 & \text{if } h < 5 \\ 1.4 & \text{if } 5 \leq h \leq 10 \\ 2 & \text{if } h > 10 \end{cases} \quad (2)$$

Table 2: Harmonic current injection data.

$h$	Load $I_h/I_r$ (%)	PV $I_h/I_r$ (%)	WTG $I_h/I_r$ (%)	$h$	Load $I_h/I_r$ (%)	PV $I_h/I_r$ (%)	WTG $I_h/I_r$ (%)
1	100	100	100	26	-	0.04	0.02
2	-	0.11	0.10	27	-	0.02	0.02
3	0.15	0.15	0.10	28	-	0.08	0.02
4	-	0.10	0.10	29	0.11	0.05	0.03
5	0.37	0.16	0.40	30	-	0.05	0.01
6	-	0.03	0.14	31	-	0.11	0.02
7	0.28	0.18	0.07	32	-	0.05	0.01
8	-	0.04	0.06	33	-	0.02	0.02
9	0.27	0.04	0.05	34	0.09	0.03	0.02
10	-	0.04	0.04	35	0.09	0.03	0.04
11	0.41	0.12	0.06	36	-	0.00	0.04
12	-	0.01	0.03	37	-	0.02	0.04
13	0.12	0.11	0.05	38	-	0.01	0.06
14	-	0.03	0.02	39	-	0.08	0.06
15	-	0.02	0.02	40	-	0.10	0.06
16	-	0.02	0.01	41	-	0.13	0.05
17	0.16	0.06	0.03	42	-	0.02	0.10
18	-	0.04	0.01	43	-	0.08	0.10
19	0.08	0.05	0.03	44	-	0.08	0.10
20	-	0.02	0.01	45	-	0.10	0.10
21	0.08	0.02	0.01	46	-	0.02	0.10
22	-	0.02	0.01	47	-	0.11	0.10
23	0.60	0.07	0.02	48	-	0.10	0.10
24	-	0.01	0.01	49	-	0.13	0.10
25	0.08	0.09	0.02	50	-	0.01	0.10

Notation ' $h$ ' denotes the harmonic order, ' $I_h$ ' and ' $I_r$ ' refer to harmonic current at order  $h$  and reference current, respectively.

where  $I_h$  is the harmonic current at  $h^{th}$  harmonic order,  $N$  is the number devices connected at PCC and  $\alpha$  is the summation exponents for different harmonic orders.

For modelling the UPC current harmonic sources, the harmonic current amplitudes of three phases were set to be identical to allow comparisons with the IEC model. The actual three-phase harmonic phase angles of the UPC model are calculated as  $\varphi_h^A = \Delta\varphi_h^A + h\varphi_1^A$ ,  $\varphi_h^B = \Delta\varphi_h^B + h\varphi_1^B$  and  $\varphi_h^C = \Delta\varphi_h^C + h\varphi_1^C$  (DIGSILENT, 2020b), where  $h$  is the harmonic order, and  $\varphi_1^A$ ,  $\varphi_1^B$  and  $\varphi_1^C$  are the fundament current angles of phase A, B and C, respectively. The phase parameters  $\Delta\varphi_h^A$ ,  $\Delta\varphi_h^B$  and  $\Delta\varphi_h^C$  used to specify each harmonic phase angle were set to 0 for positive (e.g. 4, 7, 10, ...) and negative-sequence (e.g. 2, 5, 8, ...) orders. Since the triplen harmonics in IEC source are considered as positive-sequence, the  $\Delta\varphi_h^A$ ,  $\Delta\varphi_h^B$  and  $\Delta\varphi_h^C$  in UPC model were set to 0, -120 and 120, respectively to enable modelling of zero-sequence components (i.e. triplen harmonics) to be considered as positive-sequence as in the IEC model. Therefore, the UPC harmonic source is effectively modelled as a balanced harmonic model, similar to the IEC

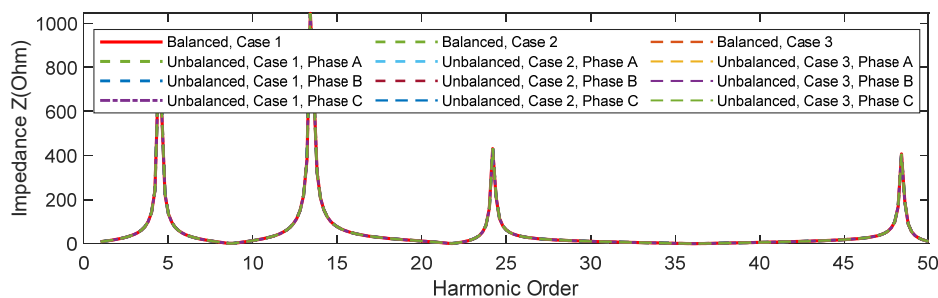


Figure 2: Balanced and unbalanced impedance characteristics at B2 for Case 1, Case 3 and Case 3.

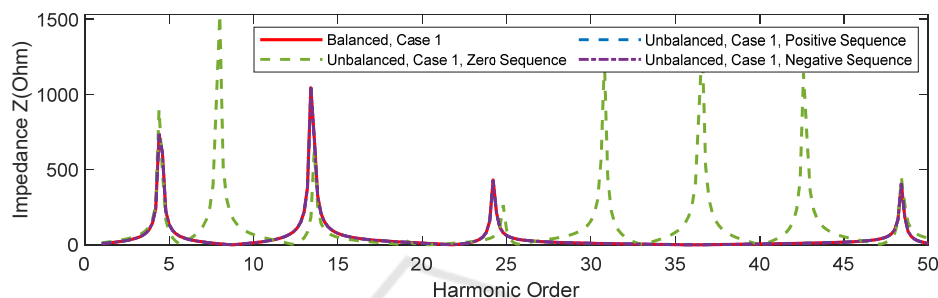


Figure 3: Balanced and unbalanced impedance characteristics at B2 of Case 1.

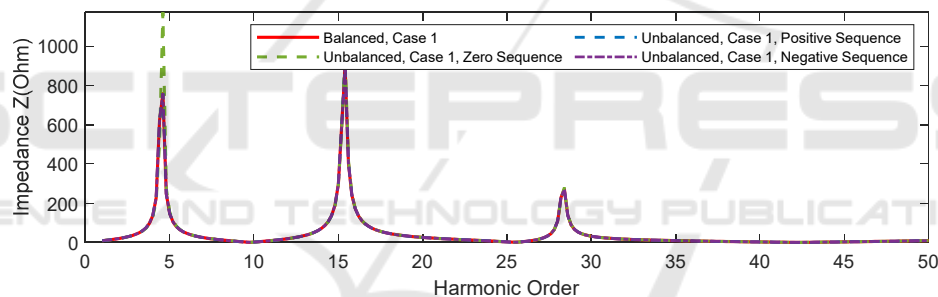


Figure 4: Balanced and unbalanced impedance characteristics at B2 of Case 1 under ideal system conditions.

harmonic source, so that the results from the two models can be compared.

### 3 SIMULATION RESULTS AND DISCUSSION

This section first presents impedance characteristics obtained from balanced and unbalanced frequency sweep analysis when IEC and UPC model are used. Then, various harmonic load flow calculations are performed using different solvers, to compare the voltage THD values and examine the differences between the IEC and the UPC model. Finally, the possibility of matching the IEC model using an equivalent UPC model is studied and discussed.

#### 3.1 Frequency Scan Analysis

The frequency scan analysis can be seen as solving the network equation  $I^h = Y^h V^h$  (Medina et al., 2013). where  $I^h$ ,  $V^h$  and  $Y^h$  are current vector, voltage vector and admittance matrix at harmonic order  $h$ , respectively. Injecting one pu current and calculating the corresponding voltage, the system admittance is obtained. Under the assumption of system linearity, the frequency scan analysis always produces the same impedance characteristics regardless harmonic injection values, the type of harmonic source model and the number of harmonic sources. The approach described above is used by DPF and other commercial software to calculate the system impedance. In order to verify this assumption, the balanced and unbalanced frequency scans were

calculating by injecting 10 Hz step size harmonic current up to 2.5 kHz, under following cases:

- Case 1: IEC model adopted for 3 loads, 2 PVs and 2 WTGs.
- Case 2: UPC model adopted for the 3 loads, 2 PVs and 2 WTGs.
- Case 3: no harmonic source model is considered.

The impedance characteristics at the 132 kV busbar B2 for the different cases are presented in Figure 2. The frequency response at B2 for the tested cases was exactly the same no matter the type and number of harmonic sources, and the selection of balanced or unbalanced frequency scan. These findings were also verified to other busbars.

In addition to above tests, the impedance characteristics between balanced and unbalanced components are compared, as shown in Figure 3. Although Figure 3 only shows the frequency characteristics of Case 1, the same results were found for Case 2 and 3. It can be seen that the balanced, unbalanced positive-sequence and negative-sequence share the same impedance characteristics, and their resonance frequencies occur at the 4<sup>th</sup>, 13<sup>rd</sup>, 24<sup>th</sup> and 48<sup>th</sup> orders. This is because the balanced frequency scan in DPF considers the positive-sequence component only. The resonance frequency of unbalanced zero-sequence shown additional resonant frequencies at the 8<sup>th</sup>, 31<sup>st</sup>, 37<sup>th</sup> and 43<sup>rd</sup> orders. These results are expected – the resonances of zero-sequence are shifted when performing unbalanced frequency scan, mostly due to the Yg-d connection of the transformers and the difference between and zero and positive/negative-sequence impedances of the network components. Based on these considerations, balanced and unbalanced frequency scans were performed under an ideal system conditions, where Yg-Yg connection was used, and positive/negative and zero-sequence impedances of the transmission lines and transformers were set to equal, with results shown in Figure 4. In this case the resonance frequencies (i.e. 5<sup>th</sup>, 15<sup>th</sup>, and 28<sup>th</sup> harmonic orders) of balanced and unbalanced components are identical. The same behaviour was observed for Case 2 and Case 3. It is therefore concluded that the network parameters are the only factors influencing the frequency scans.

## 3.2 Harmonic Load Flow Analysis

As reviewed in (Herraiz et al., 2003), different harmonic load flow techniques may produce distinct

results. Therefore, it is necessary to understand which technique is applied by each software in order to carry out a correct assessment. For the specific case of DPF, review of the manual (DIgSILENT, 2020b) and discussion with the technical support led to conclude that the load flow solution is calculated at fundamental frequency only, and a harmonic penetration study is carried out by applying nodal analysis at various harmonic orders. Although a ‘true’ harmonic load flow could provide more accurate results by taking into account the voltage-dependent nature of the system components, it requires significant computational effort due to the process of solving a large number of fundamental and harmonic power flow equations simultaneously (Medina et al., 2013). This may be the reason why harmonic penetration is widely used in the great majority of commercial software (Working Group JWC-C4/B4.38, 2019).

The following three cases were considered to compare the results of harmonic load flow analysis using the IEC and the UPC model, based on the selection of different harmonic load flow solvers available in DPF:

- Case 4: balanced harmonic load flow, considering positive- or negative-sequence equivalent single-phase according to default settings (positive-sequence impedance for zero- and positive-sequence harmonic orders, and negative-sequence impedance for negative-sequence harmonic orders).
- Case 5: balanced harmonic load flow with positive-sequence only (using positive-sequence impedance for all harmonic orders).
- Case 6: unbalanced harmonic load flow that considers positive or negative-sequence three-phase components at the related harmonic order.

When any IEC harmonic source model exists in the DPF model, the harmonic currents or voltages are processed using the selected harmonic summation rule (i.e. with standard or self-defined summation exponents).

### 3.2.1 Single Harmonic Source Test

In this test, the photovoltaic plant (P1) connected to the 33 kV busbar B7 was the only harmonic producing device in the network. This is a simple way to verify the differences between IEC and UPC model when different solvers are used. In Table 3, the voltage THD values at different busbars for Case 4, 5

Table 3: Comparison of THDs between IEC and UPC models under different cases (single harmonic source).

Bus	Standard IEC model		UPC model			
	Case 4&5 (%)	Case 6 3-Ph (%)	Case 4&5 (%)	Case 6 Ph-A (%)	Case 6 Ph-B (%)	Case 6 Ph-C (%)
B1	<b>0.007</b>	<b>0.007</b>	0.006	<b>0.007</b>	<b>0.007</b>	<b>0.007</b>
B2	<b>0.025</b>	<b>0.025</b>	0.023	<b>0.025</b>	<b>0.025</b>	<b>0.025</b>
B3	<b>0.031</b>	<b>0.031</b>	0.027	<b>0.031</b>	<b>0.031</b>	<b>0.031</b>
B4	<b>0.029</b>	<b>0.029</b>	0.026	<b>0.029</b>	<b>0.029</b>	<b>0.029</b>
B5	<b>0.035</b>	<b>0.035</b>	0.030	<b>0.035</b>	<b>0.035</b>	<b>0.035</b>
B6	<b>0.036</b>	<b>0.036</b>	0.032	<b>0.036</b>	<b>0.036</b>	<b>0.036</b>
B7	0.283	0.301	0.241	0.297	0.307	0.292
B8	0.035	0.037	0.030	0.035	0.038	0.037
B9	<b>0.036</b>	<b>0.036</b>	0.032	<b>0.036</b>	<b>0.036</b>	<b>0.036</b>

Bold values are all the same. 'Ph-A', 'Ph-B', 'Ph-C', and '3-Phase' refer to phase A, phase B and phase C and all three phases, respectively.

Table 4: THDs for IEC and UPC models at low-voltage busbars under different cases when using Yg-yg transformers (single harmonic source).

Bus	Standard IEC model		UPC model			
	Case 4&5 (%)	Case 6 3-Ph (%)	Case 4&5 (%)	Case 6 Ph-A (%)	Case 6 Ph-B (%)	Case 6 Ph-C (%)
B7	<b>0.283</b>	<b>0.283</b>	0.241	<b>0.283</b>	<b>0.283</b>	<b>0.283</b>
B8	<b>0.035</b>	<b>0.035</b>	0.030	<b>0.035</b>	<b>0.035</b>	<b>0.035</b>

and 6 are obtained, and the following conclusions can be carried out:

- For the standard IEC model, all results are the same for Case 4, 5 and 6 (three phases), except the low-voltage busbar B7 and B8, because the use of Yg-d connection at the 132/33 kV transformers results in slightly different solutions of the fundamental load flow for Case 6. By changing the 132/33 kV transformers to Wye grounded-wye grounded (Yg-yg) connection, the THDs at B7 and B8 are the same (bold values in Table 4).
- For the UPC model, the results for Case 4 and Case 5 are different from the IEC model because the triplen harmonics are ignored. It was verified that the results for Case 4 and Case 5 using UPC model were the same as the IEC model when the IEC model is not considering triplen harmonics.
- For the UPC model, the results for Case 6 (phase A, B and C) are the same as the IEC model, except at busbar B7 and B8. This is for a similar reason as discussed above (i.e. transformer connection resulting in slightly different fundamental power flow). Table 4 shows the same results when the transformer connection is modified.
- For all cases, the THD values at the high-voltage busbars are not affected by the transformer

Table 5: Comparison of THDs between IEC and UPC models for different cases (three harmonic sources).

Bus	Standard IEC model		UPC model			
	Case 4&5 (%)	Case 6 3-Ph (%)	Case 4&5 (%)	Case 6 Ph-A (%)	Case 6 Ph-B (%)	Case 6 Ph-C (%)
B1	<b>0.133</b>	<b>0.133</b>	0.145	0.147	0.147	0.147
B2	<b>0.520</b>	<b>0.520</b>	0.564	0.570	0.570	0.570
B3	<b>0.502</b>	<b>0.502</b>	0.546	0.557	0.557	0.557
B4	<b>0.598</b>	<b>0.598</b>	0.640	0.648	0.648	0.648
B5	<b>0.657</b>	<b>0.657</b>	0.692	0.705	0.705	0.705
B6	<b>0.638</b>	<b>0.638</b>	0.677	0.689	0.689	0.689
B7	3.174	3.178	3.148	3.328	3.339	3.311
B8	0.657	0.658	0.692	0.705	0.706	0.705
B9	<b>0.638</b>	<b>0.638</b>	0.676	0.689	0.689	0.689

Table 6: Comparison of THDs between IEC and UPC models for different cases (three harmonic sources).

Bus	Self-defined IEC Model		UPC Model assessed by standard IEC summation rule			
	Case 4&5 (%)	Case 6 3-Ph (%)	Case 4&5 (%)	Case 6 Ph-A (%)	Case 6 Ph-B (%)	Case 6 Ph-C (%)
B1	0.160	0.160	0.134	0.136	0.136	0.136
B2	0.620	0.620	0.525	0.530	0.530	0.530
B3	0.611	0.611	0.505	0.515	0.515	0.515
B4	0.698	0.698	0.601	0.608	0.608	0.608
B5	0.753	0.753	0.656	0.669	0.669	0.669
B6	0.745	0.745	0.639	0.650	0.650	0.650
B7	3.437	3.495	3.128	3.273	3.278	3.273
B8	0.753	0.757	0.656	0.668	0.669	0.668
B9	0.745	0.745	0.639	0.650	0.650	0.650

connection, the harmonic load flow solver or the harmonic source model.

- The above findings are also applicable to the cases when other loads, PVs or WTGs are considered individually.

### 3.2.2 Three Harmonic Sources at Same Busbar

In this test, P1, L3 and W1 connected at the 33 kV busbar B7 were considered as harmonic producing devices. This test helps to better understand how multiple harmonic sources are treated under different cases and models. Note that Yg-d transformers were considered in this test. In Table 5, the voltage THD values of IEC model and UPC model at different busbars under different cases are compared. The THD values obtained with the standard IEC model under different cases share similar features as presented in the single harmonic source test – the results of Case 4 and 5 were the same (the bold values in Table 5), whereas the THDs of Case 6 at B7 and B8 were slightly different from other cases. The THDs of UPC model at most busbars (except for B7 and B8) under Case 4 and 5 were same as Case 6, when triplen harmonics were not included in Case 6.

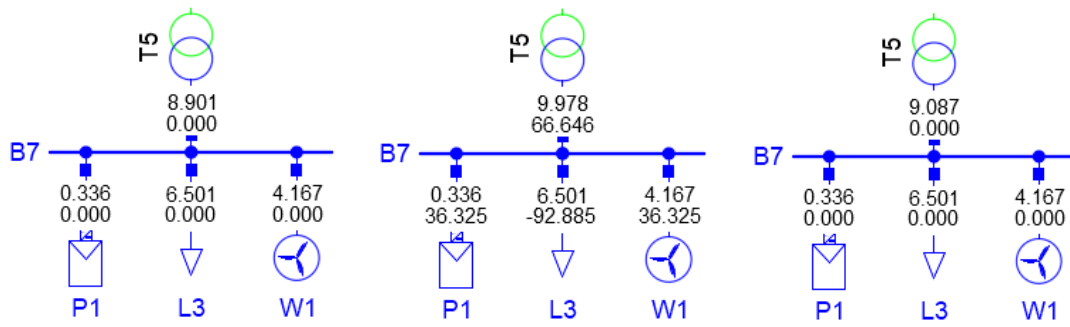


Figure 5: 5<sup>th</sup> harmonic order current flows obtained by using: the standard IEC model (left), the UPC model (middle), and the UPC model assessed by standard IEC summation rule (right).

The differences between IEC and UPC model can be explained by observing the use of summation rule, that takes the cancellation effect between harmonic sources into account.

In Table 6, the results obtained by applying IEC model under different cases using a self-defined summation exponent (i.e. value 1 was used for all frequencies) are presented. The use of the self-defined summation exponent leads to larger THDs because it assumes that all harmonics are in-phase (i.e. no cancellation effects), while the standard coefficient implies cancellation effect with increasing harmonic orders. On the other hand, in DPF, the UPC model can also be processed using the IEC summation rule, as long as one harmonic source is using IEC model. Table 6 indicates that the THDs of UPC model assessed by the standard IEC summation rule (i.e. by setting L3 to use IEC model and other two devices use UPC model) is close to the THDs obtained from using the standard IEC model (results of standard IEC model shown in Table 5). The UPC model applying the standard IEC summation rule considers both summation rule and harmonic phase angles, therefore not matching the results obtained with the standard IEC model.

To understand the causes of the discrepancies, it is worthwhile to analyse the harmonic current flows in detail. It is found that the summation of harmonic currents produced by various sources at the low-voltage side leads to different results when different summation rules and harmonic source models are applied. This is illustrated for the 5<sup>th</sup> harmonic current as shown in Figure 5, where sources P1, L3 and W1 are considered. The total harmonic current magnitude obtained for the standard IEC model is 8.901 A (i.e.  $\sqrt[1.4]{0.336^{1.4} + 6.501^{1.4} + 4.167^{1.4}}$ ); for the UPC model it is 9.978 A, obtained as  $|0.336 \angle 36.325^\circ - 6.501 \angle -92.885^\circ + 4.167 \angle 36.325^\circ|$ . Note that the harmonic current injection of the load element of UPC source model is considered in an opposite

direction of the IEC source model in DPF. The last case in Figure 5 shows the UPC model assessed by the standard IEC rule, considering both the standard IEC summation exponent and the UPC angles, thus leading to a total harmonic current of 9.087 A (i.e.  $\sqrt[1.4]{|0.336 \angle 36.325^\circ + 4.167 \angle 36.325^\circ|^{1.4} + 6.501^{1.4}}$ ). When the self-defined summation exponent was used, the above current flow equations were changed accordingly.

Given the above results, the UPC model considering harmonic phase angles may be preferable under some circumstances, because it allows modelling the harmonic phase angles in a flexible way. On the contrary, the IEC model using the standard summation exponent may put emphasis on harmonic cancellation, while the phase angles are fixed. Therefore, the UPC model will generally not match exactly the standard IEC model, even if the standard IEC summation rule is applied to the UPC model. By adjusting the settings, the UPC model will lead to results that are comparable to the IEC model, as discussed in the next section.

### 3.2.3 Matching IEC and Equivalent UPC Harmonic Current Model

After identifying the sources of discrepancies, the following settings are proposed to improve the match between the IEC model and the UPC model:

- The in-phase UPC model needs to be set as follows: the three-phase angles (i.e.  $\varphi_h^A$ ,  $\varphi_h^B$  and  $\varphi_h^C$ ) of positive-sequence and triplen orders in UPC model are set to  $0^\circ$ ,  $-120^\circ$  and  $120^\circ$ , while  $0^\circ$ ,  $120^\circ$  and  $-120^\circ$  are used for negative-sequence orders. The use of such in-phase UPC harmonic source model will not consider harmonic cancellation effect and will ensure that the same amount of harmonic current injections is obtained when multiple



Table 7: THD results for self-defined IEC and in-phase UPC modes under different study cases when using Yg-yg transformers.

Three harmonic sources				
Bus	Self-defined IEC Model		In-Phase UPC Model	
	Case 4,5,6 (%)	Case 4*,5*,6* (%)	Case 4,5,6* (%)	Case 6 3-Ph (%)
B1	<b>0.160</b>	0.158	0.158	<b>0.160</b>
B2	<b>0.620</b>	0.613	0.613	<b>0.620</b>
B3	<b>0.611</b>	0.600	0.600	<b>0.611</b>
B4	<b>0.698</b>	0.690	0.690	<b>0.698</b>
B5	<b>0.753</b>	0.740	0.740	<b>0.753</b>
B6	<b>0.745</b>	0.732	0.732	<b>0.745</b>
B7	<b>3.437</b>	3.261	3.261	<b>3.437</b>
B8	<b>0.753</b>	0.740	0.740	<b>0.753</b>
B9	<b>0.745</b>	0.732	0.732	<b>0.745</b>

Seven harmonic sources				
Bus	Self-defined IEC Model		In-Phase UPC Model	
	Case 4,5,6 (%)	Case 4&6* (%)	Case 5 (%)	Case 6 3-Ph (%)
B1	0.257	0.243	0.243	0.248
B2	1.001	0.918	0.918	0.931
B3	1.008	0.934	0.935	0.960
B4	1.110	0.987	0.986	1.005
B5	1.166	0.998	1.000	1.030
B6	1.176	1.015	1.016	1.044
B7	3.647	3.196	3.201	3.391
B8	1.328	1.028	1.028	1.114
B9	1.371	1.046	1.046	1.172

Note the cases with ‘\*’ label refer to the triplen harmonics are not considered.

harmonic sources are connected to same busbar (i.e. similarly to the IEC model assessed by self-define IEC summation rule).

- The magnitude of the harmonic currents in the UPC model is required to be set to a negative value when modelling a load element.
- The Yg-yg transformer connection is needed to avoid discrepancies at low-voltage busbars. For example, different three-phase THD values of UPC model for Case 6, and different THDs of IEC and UPC models obtained from different harmonic load flow solvers, as discussed in 3.2.1

By using the settings above for the three harmonic sources test, using the self-defined IEC and in-phase UPC models lead to the same harmonic current injection propagating to the upstream network. As shown in Table 7 (bold values), the THDs obtained from using in-phase UPC model are same to the self-defined IEC model, except the UPC model under Case 4 and 5 (because these cases are ignoring the triplen harmonics). When triplen harmonics were

Table 8: THDs of self-defined IEC and in-phase UPC models for different cases when length of transmission lines and phase-shift of transformers are set to zero and using Yg-yg transformers (seven harmonic sources).

Bus	Self-defined IEC Model	In-Phase UPC Model*		In-Phase UPC Model	
	Case 4,5,6 (%)	Case 4,5,6* (%)	Case 6 3-Ph (%)	Case 4,5,6* (%)	Case 6 3-Ph (%)
B1	<b>0.387</b>	0.368	<b>0.387</b>	0.366	<b>0.387</b>
B2	<b>1.518</b>	1.444	<b>1.518</b>	1.439	<b>1.518</b>
B3	<b>1.518</b>	1.444	<b>1.518</b>	1.439	<b>1.518</b>
B4	<b>1.518</b>	1.444	<b>1.518</b>	1.439	<b>1.518</b>
B5	<b>1.518</b>	1.444	<b>1.518</b>	1.439	<b>1.518</b>
B6	<b>1.518</b>	1.444	<b>1.518</b>	1.439	<b>1.518</b>
B7	<b>4.974</b>	4.748	<b>4.974</b>	4.708	<b>4.974</b>
B8	<b>1.854</b>	1.723	<b>1.854</b>	1.719	<b>1.854</b>
B9	<b>1.992</b>	1.813	<b>1.992</b>	1.808	<b>1.992</b>

‘In-phase UPC model\*’ means the UPC model is assessed by self-defined summation rule, and the ‘6\*’ is the case 6 without considering triplen harmonics.

ignored in the IEC models, the THDs were same to the UPC model under different cases (see Table 7).

When seven harmonic sources – 3 loads, 2 PVs and 2 WTGs – located at different busbars were considered, the THD values of self-defined IEC and in-phase UPC model were not matching although the differences were small (see Table 7). Note that the THDs of in-phase UPC model under Case 5 were not exactly the same as in Case 4 and Case 6\*, because the solver in Case 5 considers positive-sequence impedance for all harmonic orders.

Nevertheless, it is possible to match the results obtained from the IEC model with the self-defined summation exponent (i.e. 1 for all frequencies) by using the proposed in-phase model if the length of the transmission lines and the phase-shift of the transformers are considered to be zero. In this way, the diversity due to the network impedance is not considered, therefore the comparison between different harmonic modelling approaches and harmonic load flow solvers is straightforward. The voltage THD results in Table 8 show that the use of in-phase UPC model produce the same THDs (the bold values) as the use of self-defined IEC model for Case 6 under the specified system conditions. Moreover, Table 8 shows that the UPC model assessed by IEC summation rule with self-defined summation exponent (i.e. ‘In-Phase UPC\*’) is able to produce the same result for Case 6 (see bold values in Table 8). The differences between In-Phase UPC and In-Phase UPC under Case 4, 5 and 6\* are because the device L3 in the case In-Phase UPC\* was using IEC model that takes triplen harmonics into account.

Based on the results above, even with the proposed settings, the in-phase UPC model does not allow exact match of the IEC model results obtained by applying the standard summation rule when

multiple harmonic sources are located at different busbars. This is because the UPC model takes into account the cancellation caused by the network impedance (i.e. superposition law): more specifically, it was found that the harmonics propagating to the network through the transmission lines and phase-shifting transformers result in harmonic phase shift when using the UPC model. On the contrary, the standard IEC model summation rule accounts for the effect of harmonic cancellation from the harmonic source injections and the effect of network impedance, irrespective of the transformer phase shift.

## 4 CONCLUSIONS

This paper addressed different approaches in modelling unbalanced systems with large penetration of RESs for the purpose of harmonic studies. Two aspects were considered: frequency scans and harmonic penetration studies.

The frequency scans indicated that the single-phase and three-phase network impedance characteristics were not affected by the harmonic models and the number of harmonic sources, as well as the use of balanced and unbalanced solver.

Various harmonic settings in DPF were tested to solve harmonic power flow using the IEC and UPC model. The discrepancies caused by the two models and harmonic load flow solvers have been analysed and clarified by comparing different cases. In addition, the possibility and requirement of modelling equivalent IEC model by using the UPC model have been proposed and verified.

Finally, it was concluded that the UPC model and the unbalanced harmonic load flow should be considered for harmonic analysis for certain operating conditions, for example (1) in stochastic harmonic analysis, (2) where it is deemed that the generic IEC summation rule may lead to underestimation or overestimation of harmonic levels, as it assumes a 'standard' cancellation of harmonic that may not take place in the practice. When power converter-based devices, such as RESs, are considered, it is recommended to adopt the UPC model that accurately considers harmonic magnitude and phase. In this way, the harmonic cancellation effect is considered properly, and thus the harmonic assessment is more accurate and reliable.

Future work will include: developing a frequency-dependent Norton admittance model to be used with the UPC harmonic current source; applying this model to a larger network representing a portion of the UK transmission grid and studying increasing

levels of RESs and their impact on harmonic levels on the system.

## ACKNOWLEDGEMENTS

The authors acknowledge the support of the UK Engineering and Physical Sciences Research Council (EPSRC); Project EP/T013206/1.

## REFERENCES

- Ambrož, B., Boštjan, B., Aljaž, Š., Mari, L., Jako, K., & Kai, S. (2017). Simulation Models for Power-Quality Studies in Power-Electronics Rich Power Networks-Deliverable 5.2. *MIGRATE – Massive InteGRATion of Power Electronic Devices*, 1–323.
- Bećirović, E., Jovica, V. M., Simon, H., Maren, K., Kai, S., & Dejan, M. (2018). Propagation of PQ disturbances Through The Power Networks - Deliverable 5.3. *MIGRATE – Massive InteGRATion of Power Electronic Devices*, 1–154.
- Cherian, E., Bindu, G. R., & Chandramohan, P. S. (2016). Pollution Impact of Residential Loads on Distribution System and Prospects of DC Distribution. *Engineering Science and Technology, an International Journal*, 19(4), 1655–1660.
- DIgSILENT. (2020a). *PowerFactory 2020*. <https://www.digsilent.de/en/powerfactory.html>
- DIgSILENT. (2020b). *PowerFactory 2020 User Manual*. 889–906. <https://www.digsilent.de/en/powerfactory.html>
- Elkholly, A. (2019). Harmonics Assessment and Mathematical Modeling of Power Quality Parameters for Low Voltage Grid Connected Photovoltaic Systems. *Solar Energy*, 183, 315–326.
- Eltouki, M., Rasmussen, T. W., Guest, E., Shuai, L., & Kocewiak, Ł. (2018). Analysis of Harmonic Summation in Wind Power Plants Based on Harmonic Phase Modelling and Measurements. *17th International Wind Integration Workshop*, 1–7.
- Energy Networks Association. (2020). Harmonic Voltage Distortion and the Connection of Non-Linear and Resonant Plant and Equipment to Transmission Systems and Distribution Networks in the United Kingdom. *ENA Engineering Recommendation G5*, 5.
- Energyforsk. (2018). Harmonics and Wind Power. *Daphne Schwanz, Math Bollen, Lulea University of Technology*, 1–42.
- Erik, J., & Leigh, S. H. (2016). Power Quality Assessment of Solar Photovoltaic Inverters. *Sustainable Technologies Evaluation Program, Toronto and Region Conservation Authority, Toronto, Ontario*, 1–58.
- Ghassemi, F., & Koo, K. (2010). Equivalent Network for Wind Farm Harmonic Assessments. *IEEE Transactions on Power Delivery*, 25(3), 1808–1815.

- Herraiz, S., Sainz, L., & Clua, J. (2003). Review of Harmonic Load Flow Formulations. *IEEE Transactions on Power Delivery*, 18(3), 1079–1087.
- IEC TR 61000-3-6. (2008). *Electromagnetic Compatibility, Limits – Assessment of Emission Limits for The Connection of Distorting Installations to MV, HV and EHV Power Systems*.
- IEEE Power and Energy Society. (2014). IEEE Recommended Practice and Requirements for Harmonic Control in Electric Power Systems. *IEEE Std. 519-2014*.
- Jensen, C. F. (2018). Harmonic Background Amplification in Long Asymmetrical High Voltage Cable Systems. *Electric Power Systems Research*, 160, 292–299.
- Koo, K. L., & Emin, Z. (2016). Comparative Evaluation of Power Quality Modelling Approaches for Offshore Wind Farms. *5th IET International Conference on Renewable Power Generation (RPG)*, 1–7.
- Medina, A., Segundo, J., Ribeiro, P., Xu, W., Lian, K. L., Chang, G. W., Dinavahi, V., & Watson, N. R. (2013). Harmonic Analysis in Frequency and Time Domain. *IEEE Transactions on Power Delivery*, 28(3), 1813–1821.
- Mendonça, G. A., Pereira, H. A., & Silva, S. R. (2012). Wind Farm and System Modelling Evaluation in Harmonic Propagation Studies. *Renewable Energy and Power Quality Journal*, 1(10), 647–652.
- National Grid ESO. (2019). *Future Energy Scenarios 2019*. <http://fes.nationalgrid.com/fes-document/>
- Oliver, A., Liam, M., Griffiths, F., Shafiu, A., & Forooz, G. (2018). Subgroup Report – Harmonics Above 50th. *ENA Engineering Recommendation G5*.
- Preciado, V., Madrigal, M., Muljadi, E., & Gevorgian, V. (2015). Harmonics in A Wind Power Plant. *IEEE Power and Energy Society General Meeting*, 1–5.
- Preda, T. N., Uhlen, K., & Nordgard, D. E. (2012). Instantaneous Harmonics Compensation Using Shunt Active Filters in A Norwegian Distribution Power System With Large Amount of Distributed Generation. *3rd IEEE International Symposium on Power Electronics for Distributed Generation Systems (PEDG)*, 153–160.
- Rampinelli, G. A., Gasparin, F. P., Bühler, A. J., Krenzinger, A., & Chenlo Romero, F. (2015). Assessment and Mathematical Modeling of Energy Quality Parameters of Grid Connected Photovoltaic Inverters. *Renewable and Sustainable Energy Reviews*, 52, 133–141.
- Rauma, K. (2012). Electrical Resonances and Harmonics in a Wind Power Plant. In *Aalto University School of Electrical Engineering Kalle*.
- Robinson, D. (2003). *Harmonic Management in MV Distribution Systems*. University of Wollongong.
- Working Group JWC-C4/B4.38. (2019). Network Modelling for Harmonic Studies. *CIGRE*, 1–241.
- Working Group JWG-C4/C6.29. (2016). Power Quality Aspects of Solar Power. *CIGRE*, 1–109.